HHS Public Access

Author manuscript

Circ Res. Author manuscript; available in PMC 2022 January 08.

Published in final edited form as:

Circ Res. 2021 January 08; 128(1): 76–88. doi:10.1161/CIRCRESAHA.120.317839.

Adrenergic $Ca_V1.2$ Activation via Rad Phosphorylation Converges at α_{1C} I-II Loop

Arianne Papa[a,b,*], **Jared Kushner**[a,*], **Jessica A. Hennessey**[a], **Alexander N. Katchman**[a], **Sergey I. Zakharov**[a], **Bi-xing Chen**[a], **Lin Yang**[a], **Ree Lu**[a], **Stephen Leong**[a], **Johanna Diaz**[b], **Guoxia Liu**[a], **Daniel Roybal**[a,c], **Xianghai Liao**[a], **Pedro J. del Rivero Morfin**[b], **Henry M. Colecraft**[b,c], **Geoffrey S. Pitt**[d], **Oliver Clarke**[b], **Veli Topkara**[a], **Manu Ben-Johny**[b], **Steven O. Marx**[a,c]

[a]Division of Cardiology, Department of Medicine, Columbia University, Vagelos College of Physicians and Surgeons, New York, NY 10032

[b]Department of Physiology and Cellular Biophysics

[c]Department of Pharmacology and Molecular Signaling, Columbia University, Vagelos College of Physicians and Surgeons

[d]Cardiovascular Research Institute, Weill Cornell Medical College.

Abstract

Rationale: Changing activity of cardiac $Ca_V1.2$ channels under basal conditions, during sympathetic activation, and in heart failure is a major determinant of cardiac physiology and pathophysiology. Although cardiac $Ca_V1.2$ channels are prominently up-regulated via activation of protein kinase A, essential molecular details remained stubbornly enigmatic.

Objective: The primary goal of this study was to determine how various factors converging at the $Ca_V1.2$ I-II loop interact to regulate channel activity under basal conditions, during β-adrenergic stimulation, and in heart failure.

Methods and Results: We generated transgenic mice with expression of $Ca_V1.2$ α_{1C} subunits with: 1) mutations ablating interaction between α_{1C} and β subunits; 2) flexibility-inducing polyglycine substitutions in the I-II loop (GGG-α_{1C}); or 3) introduction of the alternatively spliced 25-amino acid exon 9* mimicking a splice variant of α_{1C} up-regulated in the hypertrophied heart. Introducing three glycine residues that disrupt a rigid IS6-AID helix markedly reduced basal open probability despite intact binding of $Ca_V\beta$ to α_{1C} I-II loop, and eliminated β-adrenergic agonist stimulation of $Ca_V1.2$ current. In contrast, introduction of the exon 9* splice variant in α_{1C} I-II

Address correspondence to: Dr. Manu Ben-Johny, Vagelos College of Physicians and Surgeons, 622 West 168th Street, PH-3Center, New York, NY 10032, Tel: 212 305-0271, mbj2124@cumc.columbia.edu; Dr. Steven O. Marx, Vagelos College of Physicians and Surgeons, 622 West 168th Street, PH-3Center, New York, NY 10032, Tel: 212 305-0271, sm460@cumc.columbia.edu.

*contributed equally

AUTHOR CONTRIBUTIONS

Conceptualization, S.O.M.; Methodology, A.P., J.K., J.H., A.N.K., S.I.Z., M.B.J., S.O.M.; Investigation, A.P., J.K., J.H., A.N.K., S.I.Z., B.X.C., L.Y., R.L., S.L., J.D. G.L., V.T., X.L., P.M., H.M.C., G.S.P., M.B.J., S.O.M.; Writing – Original Draft, A.P., J.K., M.B.J., S.O.M.; Writing – Review & Editing, A.P., J.K., J.H., A.N.K., S.I.Z., L.Y., H.M.C., G.S.P., M.B.J., S.O.M.; Funding Acquisition, S.O.M., H.M.C., and G.S.P.; Resources, S.O.M., M.B.J, H.M.C., and G.S.P.

DISCLOSURES

None

loop, which is increased in ventricles of patients with end-stage heart failure, increased basal open probability but did not attenuate stimulatory response to β-adrenergic agonists when reconstituted heterologously with β_{2B} and Rad or transgenically expressed in cardiomyocytes.

Conclusions: Ca^{2+} channel activity is dynamically modulated under basal conditions, during β-adrenergic stimulation, and in heart failure by mechanisms converging at the α_{1C} I-II loop. $Ca_V\beta$ binding to α_{1C} stabilizes an increased channel open probability gating mode by a mechanism that requires an intact rigid linker between the β subunit binding site in the I-II loop and the channel pore. Release of Rad-mediated inhibition of Ca^{2+} channel activity by β-adrenergic agonists/PKA also requires this rigid linker and β binding to α_{1C}.

Graphical Abstract

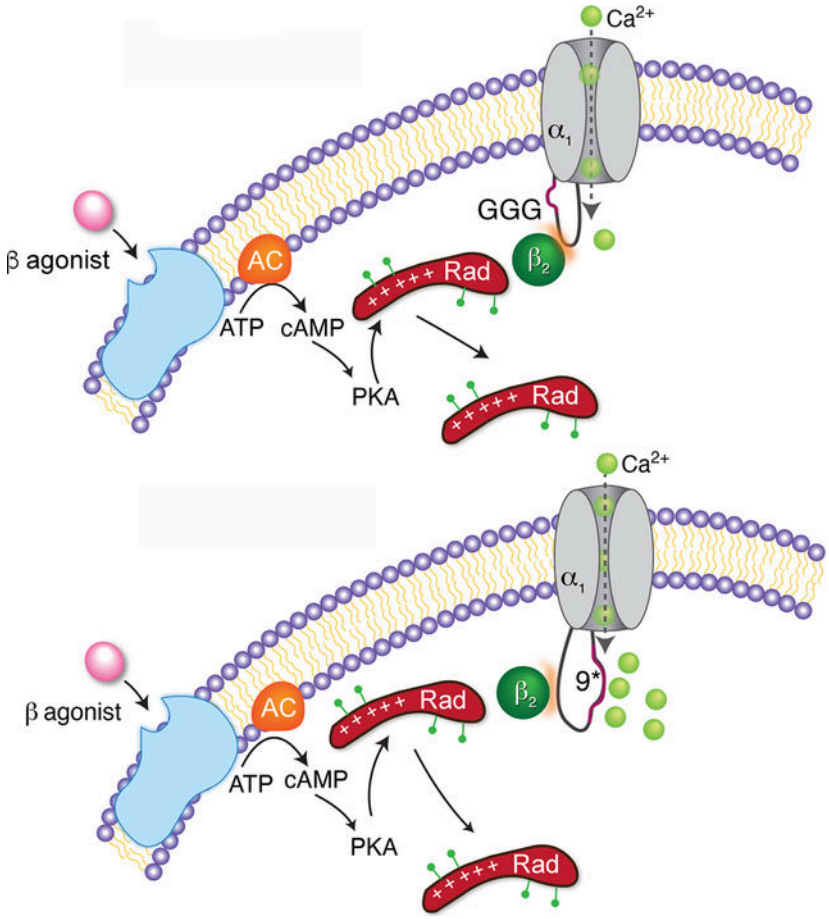

Keywords

Calcium; calcium channels; protein kinase A (PKA); adrenergic; cardiac; excitation-contraction coupling; ion channel; physiology

Subject Terms:

Basic Science Research; Calcium Cycling/Excitation-Contraction Coupling; Ion Channels/Membrane Transport; Physiology

INTRODUCTION

In cardiomyocytes, Ca^{2+} influx through L-type $Ca_V1.2$ channels commences the process of excitation-contraction coupling via the triggering of Ca^{2+} release from ryanodine receptors. In the failing heart, dysfunctional regulation of $Ca_V1.2$ channels can trigger electrical abnormalities leading to early Ca^{2+}-mediated after-depolarizations, arrhythmias, and sudden death.

Voltage-gated Ca^{2+} channels are comprised of a pore-forming α_1 subunit [1] and a cytosolic β subunit that interacts with the α-interaction domain (AID) in the intracellular linker between domains I and II (I-II loop) of the α_1 subunit [2–4] (Figure 1A). When expressed heterologously, binding to the β subunit is obligatory for α_{1C} trafficking to the plasma membrane, and for normalizing channel activation and inactivation gating properties [5–8] via a mechanism that requires a rigid IS6-AID helix linker [9, 10]. β-adrenergic agonists, via activation of protein kinase A (PKA), increase Ca^{2+} influx through $Ca_V1.2$ [11, 12], an important component of the physiological 'fight-or-flight' response that contributes to the increased contractility of the heart during exercise. The overall features of this regulation − PKA-dependent enhanced whole-cell current amplitude, a hyperpolarizing shift in voltage-dependence of channel activation, and increased open probability (P_o) − are well-established [11, 12], yet essential molecular details remained stubbornly enigmatic for decades. Recently, we showed that binding of $Ca_V\beta$ subunits to α_{1C} is required for β-adrenergic stimulation of $Ca_V1.2$ channels and positive inotropy in the heart [13], and that the Ca^{2+} channel inhibitor Rad [14], which binds to the β subunit, is the functionally relevant PKA target in the $Ca_V1.2$ complex [15].

Beyond these, the I-II loop is also subject to alternative splicing that tunes channel function and interacting proteins in a cell-type specific manner. The inclusion of alternatively-spliced exon 9* is observed at high levels in the smooth muscle and at lower but variable expression in adult heart that increases in animal models of hypertrophy and in the peri-infarct zone after myocardial infarction in mice [16–18]. This variant results in the insertion of 25 amino acid residues C-terminal to the AID [18–20] and tunes channel activation. In all, the modulatory landscape supported by the $Ca_V1.2$ domain I-II linker appears rich and multifaceted, involving the β subunits, RGK proteins, phosphoregulation by PKA, and alternative splicing, all poised to precisely tune Ca^{2+} influx into cardiomyocytes.

Several important mechanistic unknowns persist impeding in-depth pathophysiological understanding. First, although $Ca_V\beta - \alpha_1$ interaction is obligatory for $Ca_V1.2$ trafficking in heterologous cells, we found it to be dispensable for trafficking to the dyad, for basal function and for initiating excitation-contraction coupling in adult cardiomyocyte [13], thus raising fundamental questions about the functional role of $Ca_V\beta$ subunits in cardiomyocytes. Second, it is unknown how distal conformational changes involving Rad interaction with the $Ca_V\beta$ subunit and phosphorylation-dependent signaling are ultimately conveyed to the channel pore-domain. Third, how alternative splicing of the domain I-II linker contributes to this overall regulatory scheme including downstream effects of PKA activation remains to be

fully-elucidated. Importantly, the pathogenesis of heart failure has been long-suspected to reshape this regulatory framework, although the precise changes remain largely undefined.

To dissect these possibilities, we measured baseline channel gating properties and the strength of adrenergic modulation of $Ca_V1.2$ in three transgenic mouse models: (1) Our previously-established AID mutant where $Ca_V1.2$ is incapable of binding to the β subunit [13], (2) Triple-glycine substitution (GGG-α_{1C}) of the rigid I-II linker, which connects the pore-domain with the AID. These mutations have been previously shown to disrupt coupling between these two domains [9, 10, 21], and (3) The insertion of 25 amino acid residues C-terminal to the AID corresponding to the introduction of exon 9* variant (9*-α_{1C}) (Figure 1A). Our findings identify the IS6-AID linker as a vital molecular element for transducing the PKA-induced activation of $Ca_V1.2$, and as a molecular rheostat for $Ca_V1.2$ activity whereby distinct structural changes elicited by β subunits, RGK proteins, and alternative splicing bidirectionally tune Ca^{2+} influx into the heart in both normal physiology and during heart failure.

METHODS

Data Availability.

All supporting data are available within the article and its online data supplement.

For details on the experimental procedures, see the materials and methods section in the online data supplement.

RESULTS

Generation of inducible, cardiac-specific α_{1C} transgenic mice.

We created several mice lines with inducible, cardiac-specific expression of dihydropyridine (DHP)-resistant, FLAG-epitope-tagged α_{1C} (Figure 1B). We have previously shown that control transgenic FLAG-tagged DHP-resistant α_{1C} subunits, termed pseudo-wild-type α_{1C} have similar properties as native cardiac Ca^{2+} channels [22]. To study properties of $Ca_V1.2$ devoid of the β subunit, we used transgenic mice[13] expressing rabbit α_{1C} with a disrupted AID via alanine substitutions of 3 conserved residues, Y467, W470 and I471, that are essential for binding of β subunit [21]. We further generated transgenic mice (Figure 1B) expressing FLAG-tagged DHP-resistant α_{1C} with a substitution of three glycine residues (GGG) for the AKA motif in the IS6-AID linker [10], designated GGG-α_{1C} (Figure 1A). All three lines, pseudo-WT-, AID- and GGG-α_{1C} were crossed with transgenic mice expressing reverse transcriptional transactivator in the heart (αMHC-rtTA) [23] (Figure 1B), yielding mice with doxycycline-inducible α_{1C} expression. As expected, channels with a disrupted AID motif do not bind β subunits, assessed by anti-FLAG antibody immunoprecipitation of cleared homogenates (Figure 1C). By comparison, GGG-α_{1C} channels exhibit robust β subunit binding similar to pseudo-wild-type α_{1C} (Figure 1C).

Binding of β to α_{1C} enhances channel openings.

Previously, we showed that in cardiomyocytes, $Ca_V1.2$ channels without β subunits can be transported to the dyad and can generate currents that mediate normal excitation-contraction

coupling [13]. To determine whether β binding to α_{1C} alters basal channel gating in cardiomyocytes, we utilized low-noise single-channel recordings of acutely isolated cardiomyocytes, employing Ba^{2+} as a charge carrier. Stochastic channel openings, which reflect near-steady-state open probability (P_o) at each voltage, were elicted by a slow voltage ramp [24, 25]. Ca^{2+} channels in cardiomyocytes from non-transgenic mice were inhibited by 300 nM nisoldipine (Figure 1D, middle). In the transgenic mice, however, there is a mixture of transgenic nisodipine-resistant channels and endogenous nisoldipine-sensitive channels (Figure 1E–F). As dihydropyridines are known to allosterically modify channel gating [26], partial blockade of nisoldipine-resistant channels may be a confounding factor. To obviate this possibility, we obtain ~80–120 stochastic records from each patch and subsequently apply nisoldipine to identify resistant transgenic channels. This process allows us to unambiguously establish baseline function of mutant $Ca_V1.2$. Indeed, exemplar traces from DHP-resistant pseudo-wild-type α_{1C} channels confirm channel openings in the presence of nisoldipine. Measurements of steady-state P_o as a function of voltage were obtained by averaging many records and by normalizing the unitary current level. Reassuringly, steady-state P_o-V relationships of pseudo-wild-type α_{1C} channels are similar to that of non-transgenic channels. The DHP-resistant AID-mutant α_{1C} channels, however, displayed a striking 3.5-fold reduction in maximal P_o compared to DHP-sensitive endogenous Ca^{2+} channels from non-transgenic Ca^{2+} mice and DHP-resistant channels from pseudo-wild-type α_{1C} mice (Figure 1G). To further elucidate changes in elementary channel gating mechanisms, we scrutinized single-trial average open probabilities ($\bar{P}_o$) from one-channel patches. A dash-line discriminator with $\bar{P}_o = 0.1$ was used to identify low activity versus high-activity traces. Thus analyzed, pseudo-wild-type α_{1C} channels switched between epochs of no openings or blanks (40.6% of traces), low activity (33.0%), and high activity (26.4%) (Figure 1H) consistent with previous studies. By comparison, AID-mutant α_{1C} channels exhibited a distinct pattern ($p<0.0001$ by χ^2 test of independence) with rare sojourns to the high-activity mode (7.1%) and a higher propensity for blank (45.7%) and low activity sweeps (47.2%) (Figure 1I). Thus β subunit binding appears to stabilize the high-activity gating mode. We conclude that the interaction between the β subunit and the α_{1C} subunit essentially modulates $Ca_V1.2$ channel activity in cardiomyocytes by enhancing channel openings.

Increased flexibility of IS6 linker reduces basal Ca^{2+} channel activity in cardiomyocytes.

Having established the importance of β subunits in upregulating $Ca_V1.2$ channel activity, we considered whether the rigid I-II linker between the IS6 pore helix and the AID is essential for tuning channel function. Introduction of the three glycine residues in the IS6-AID linker had no effect on the subcellular localization and functional expression of $Ca_V1.2$ in cardiomyocytes. Anti-FLAG antibody immunofluorescence studies on fixed cardiomyocytes showed that GGG-α_{1C} $Ca_V1.2$ channels demonstrated a striated z-disk pattern consistent with localization to the surface membrane and transverse-tubules (t-tubules) (Figure 2A). Similar to cardiomyocytes expressing pseudo-wild-type α_{1C} or AID-mutant α_{1C} transgenic channels, field-stimulated contraction of cardiomyocytes isolated from GGG-α_{1C} transgenic mice persisted in the presence of 300 nM nisoldipine, which is sufficient to block excitation-contraction coupling induced by endogenous $Ca_V1.2$ channels in non-transgenic mice

(Figure 2B), indicating that the GGG-α_{1C} $Ca_V1.2$ channels are localized correctly and flux sufficient Ca^{2+} to evoke Ca^{2+}-induced Ca^{2+} release in cardiomyocytes.

When GGG-α_{1C} is co-expressed in *Xenopus* oocytes with β_{2B}, one of the major β_2 isoforms in the heart, channels displayed accelerated voltage-dependent inactivation but slowed Ca^{2+}-dependent inactivation [10]. Here, we assessed aggregate inactivation of Ca^{2+} channels in the heart with Ca^{2+} as a charge carrier. The inactivation kinetics of nisoldipine-resistant GGG-α_{1C} Ca^{2+} currents at +10 mV test potential was significantly faster compared to pseudo-wild-type α_{1C} controls (Figure 2C). Therefore, in adult cardiomyocytes $Ca_V1.2$ channels comprised of transgenic GGG-α_{1C} have faster overall inactivation kinetics as compared to transgenic pseudo-wild-type $Ca_V1.2$ channels likely reflecting accelerated kinetics of voltage-dependent inactivation.

Given that β subunits upregulate $Ca_V1.2$ channel P_o, we considered whether disruption of the rigid IS6-AID linker might reverse this effect. Consistent with this possibility, the conductance-voltage (*G-V*) relationships, normalized to cell capacitance, of nisoldipine-resistant transgenic mutant GGG-α_{1C} channels was reduced compared to pseudo-wild-type α_{1C} (Figure 2D). To directly assess changes in P_o, we used low-noise single-channel recordings of acutely isolated cardiomyocytes from the GGG-α_{1C} transgenic mice. Exemplar records show DHP-resistant GGG-α_{1C} channels exhibit sparse channel openings (Figure 2E, top), a distinct gating pattern compared to pseudo-wild-type α_{1C} and non-transgenic channels which undergo high-activity flickery openings (Figure 1). Ensemble average P_o-V relationship (Figure 2E, bottom) and bar-graph summary of maximal P_o (Figure 2F) from individual patches show a striking 3.5-fold reduction in maximal P_o compared to both pseudo-wild-type α_{1C} and non-transgenic channels (Figure 2F). Interestingly, this reduced basal activity of GGG-α_{1C} is reminiscent of β-less AID-mutant channels suggesting that disruption of the rigid IS6-AID linker may be akin to the uncoupling of the β subunit from the channel pore [10]. To further scrutinize this possibility, we assessed average P_o from individual trials for one channel patches of GGG-α_{1C}. Unlike pseudo-wild-type α_{1C} channels, the single-trial $\bar{P}_o$ distribution of the GGG-α_{1C} channels was restricted to either blank (73.4%) or low activity sweeps (26.6%) with no evidence of high activity traces (Figure 2G). As GGG-α_{1C} are fully capable of β subunit binding (Figure 1), these results suggest that the rigidity of the linker between the pore-domain and I-II loop may be a structural requirement for the high-activity gating configuration. As AID-mutant channels exhibit some propensity for high-activity traces, one attractive possibility is that the IS6-AID linker may switch between rigid and flexible conformations, with β subunit binding to the AID serving to stabilize the rigid helical linker conformation, an outcome also supported by X-ray crystallographic and circular dichroism experiments [2–4].

9*-α_{1C} splice variant increases basal open probability.

Having established the I-II loop as a vital regulator of channel openings, we considered whether alternative splicing in this domain might tune channel gating. The 9* exon, which encodes a 75-nucleotide sequence within the I-II loop (Figure 3A), is expressed at a high level in aortic smooth muscle and has lower expression in non-diseased adult human and rat heart. However, the 9* exon-containing channels are increased in rodent models of

hypertrophy and in the perinfarct zone [16–18]. This altered pattern of α_{1C} splicing in rodent models raises the possibility of pathological inclusion of exon 9* in human cardiac disease, an outcome yet to be observed clinically. As such, we sought to determine whether the frequency of exon 9* splice variant is changed in humans with end-stage heart failure. Samples from patients undergoing LVAD implantation at Columbia-NY Presbyterian Hospital were acquired in the operating room, and compared to samples obtained from donor hearts without heart failure (Online Tables I–III). Exon 9* transcript expression was increased in humans with heart failure compared to control samples (Figure 3B).

To determine the functional consequence of exon 9* splice inclusion in cardiomyocytes, we created transgenic mice with cardiac-specific expression of DHP-resistant Ca^{2+} channels containing exon 9*, but with all other mutually exclusive exons typical of cardiac variants. The 9*-α_{1C} channels still bound β subunits (Figure 3C) similar to pseudo-wild-type α_{1C} channels, and trafficked to the surface membrane and t-tubules, as demonstrated by the striated z-disk pattern of immunofluorescence (Figure 3D). Whole-cell electrophysiological analysis of nisoldipine-resistant transgenic mutant 9*-α_{1C} channels revealed a signicant increase in the *G-V* relationship normalized to cell capacitance in comparison to pseudo-wild-type α_{1C} channels (Figure 3E). Changes in whole cell current may stem from alterations in channel trafficking, unitary conductance, or baseline open probability. To dissect these mechanistic possibilities, we undertook low-noise single-channel recordings to determine whether the increased normalized conductance of 9*-α_{1C} reflected a genuine increase in channel P_o. In the presence of nisoldipine, the DHP-resistant 9*-α_{1C} channels exhibited robust channel openings (Figure 3F) with the ensemble average demonstrating a marked increase in maximal P_o (0.26 ± 0.03, mean ± s.e.m) (Figure 3G) in comparison to pseudo-wild-type α_{1C} (0.15 ± 0.015, mean ± s.e.m). Furthermore, examination of single-trial $\bar{P}_o$ distribution revealed a virtual elimination of blank traces (~0% for 9* versus 40.5% for pseudo-wild-type α_{1C} -see Figure 1H), and increased propensity for the high activity gating mode (56.7%) (Figure 3H). Thus, the insertion of the 9* exon into the I-II loop upregulates basal voltage-dependent opening of Ca^{2+} channels by enhancing channel availability and stabilizing the high P_o gating configuration. Interestingly, this functional signature is reminiscent of $Ca_V1.2$ behavior in myocytes from failing human hearts, which also show increased availability and P_o [27].

β-adrenergic upregulation of $Ca_V1.2$ also requires a rigid IS6-AID linker.

Recently, we determined that the mechanism of adrenergic stimulation of $Ca_V1.2$ requires constitutive pre-inhibition of $Ca_V1.2$ mediated by Rad interaction with the Ca_V channel β subunit [15]. PKA phosphorylation of Rad at conserved sites in its C-terminus alters its interaction with the Ca_V channel β subunit and relieves constitutive inhibition [15]. As increased flexibility of the IS6-AID linker effectively decouples β subunit mediated regulation, we hypothesized that the rigid IS6-AID linker may be also essential for adrenergic upregulation of $Ca_V1.2$ currents. Consistent with this possibility, at the single channel level, Rad inhibited $Ca_V1.2$ channels have decreased availability and increased propensity for low activity gating mode, akin to GGG-α_{1C} channels [9, 10].

In cardiomyocytes isolated from mice expressing transgenic pseudo-wild-type α_{1C}, forskolin (an adenylyl cyclase activator) induced an increase in the nisoldipine-insensitive maximal conductance (G_{max}) (Figure 4A–B, G), and shifted the V_{50} for activation (Figure 4H), consistent with our prior studies [13, 22, 28, 29]. Ca^{2+} currents through transgenic GGG-α_{1C} channels, however, were not stimulated by forskolin (Fig 4C–D, G–H). By comparison, forskolin increased the G_{max} of 9* exon-containing $Ca_V1.2$ channels by a mean of 1.4-fold (Fig 4E–F, G), and shifted the V_{50} for activation (Figure 4H) suggesting that the 9* exon still preserves responsiveness to PKA modulation. For both pseudo-wild-type α_{1C} and 9* $Ca_V1.2$ channels, the forskolin-induced enhancement of Ca^{2+} current was greatest at hyperpolarized potentials and decreased as the test potential approached the reversal potential of Ca^{2+} (Figure 4I), consistent with prior observations [12]. The GGG $Ca_V1.2$ channels failed to respond to forskolin at any test potential (Figure 4I).

We used reconstitution studies in HEK293T cells [15] to further gain insights into the mechanisms by which the β subunit and I-II loop modulate adrenergic regulation of $Ca_V1.2$. In cells transfected with only α_{1C} + β_{2B}, superfusion of forskolin did not affect the Ba^{2+} currents (Figure 5A). In contrast, applying forskolin to cells expressing α_{1C} + β_{2B} + Rad increased the current as we have previously described [15]. Consistent with our findings in cardiomyocytes, in cells transfected with GGG-α_{1C} forskolin failed to increase G_{max} or shift the voltage-dependence of activation in a hyperpolarizing direction (Figure 5C–D, G–H). In contrast, applying forskolin to cells expressing 9*-α_{1C}, β_{2B}, and Rad increased the G_{max} by a mean of 1.6-fold, and shifted the V_{50} for activation (Figure 5E–H).

Flow-cytometry Förster resonance energy transfer (FRET) 2-hybrid assay [30] was utilized to determine whether the presence of GGG substitutions or 9* exon altered β subunit binding to the I-II loop, which is required for β-adrenergic regulation of $Ca_V1.2$ in heart [13] or the PKA-induced reduction in Rad binding to the β_{2B} subunit. Robust interaction is detected between Cerulean-tagged β_{2B} subunit and Venus-tagged I-II loop (Online Figure I A, E). As would be expected, the mutation of the AID of the I-II loop markedly reduced binding (Online Figure I B), whereas the GGG substitutions or insertion of the 9* exon did not affect binding (Online Figure I C–E). As we previously reported [15], there is a strong interaction between the Cerulean-tagged β_{2B} subunit and Venus-tagged WT Rad (Online Figure II A–B,K). This interaction was markedly weakened, however, by co-expression of PKA catalytic subunit. The basal and PKA-dependent reduction of binding between Rad and β_{2B} was unaffected by co-expression of WT α_{1C} (Online Figure II C–D,K). Similarly, expression of the AID-mutant α_{1C} (Online Figure II E–F), GGG-α_{1C} (Online Figure II G–H) or 9*-α_{1C} (Online Figure II I–J) had no effect on the basal or the PKA-dependent reduction in binding between Rad and β_{2B} (Online Figure II K). These results suggest that the PKA-dependent dissociation of Rad and β_{2B} is neither dependent upon the binding of β to α_{1C} nor is it perturbed by the alterations in the I-II loop induced either by the GGG substitution or insertion of the 9* exon.

DISCUSSION

This work has examined mechanisms of regulation of cardiac $Ca_V1.2$ channel gating by three essential factors with important physiological and pathophysiological consequences

that converge at the α_{1C} subunit I-II loop— auxiliary $Ca_V\beta$ subunits, sympathetic activation, and alternative splicing. Overall, we find that PKA-modulation of Ca_V channels in heart and HEK cells is dependent on both Rad phosphorylation and a rigid IS6-AID linker. We discuss our findings on these three inter-related regulatory mechanisms in the context of previously published reports.

Many reconstitution studies in heterologous mammalian cells established the idea that auxiliary $Ca_V\beta$ subunits were necessary for trafficking of $Ca_V1.2$ channels to the plasma membrane, and that this depended on high-affinity $Ca_V\beta$ binding to a discrete α_1-interaction domain (AID) in the α_{1C} I-II loop [5, 7, 31–37]. Beyond trafficking, $Ca_V\beta$ binding also boosted $Ca_V1.2$ P_o and produced a hyperpolarizing shift in the voltage-dependence of channel activation [36, 38]. These gating effects were deduced to require formation of a rigid helix spanning IS6 and AID because they were selectively eliminated by a triple glycine substitution that disrupts the continuous helix [10]. In adult cardiomyocytes, cardiac-specific excision of the dominant cardiac $Ca_V\beta_2$ isoform reduced β_2 protein levels by 96%, yet resulted in only a 26% reduction in whole-cell $Ca_V1.2$ current, providing a first hint that, by contrast to heterologous cells, $Ca_V\beta$ binding to α_{1C} may not be obligatory for forming functional $Ca_V1.2$ channels at the cell surface [39]. We explicitly confirmed this by showing that transgenic mice expressing a DHP-resistant α_{1C} mutant that does not bind $Ca_V\beta$, nevertheless, yielded robust nisoldipine-resistant whole-cell Ca^{2+} currents indicating that the channels made it to the surface sarcolemma [29,13]. While $Ca_V\beta$ does not appear necessary for surface trafficking of $Ca_V1.2$ in adult cardiomyocytes, it remained unclear whether this also extended to the impact on channel P_o. Here, we unambiguously show using single-channel recordings that $Ca_V\beta$ binding to α_{1C} in cardiomyocytes enhances $Ca_V1.2$ channel P_o by 3.5-fold. The single-channel gating signature of AID-mutant channels was dominated by null (46%) and low-activity (47%) sweeps, with rare sojourns into a high-activity (7%) gating mode. By contrast, $Ca_V\beta$-bound pseudo-WT channels displayed more high-activity sweeps (26%) and correspondingly lower null (41%) and low-activity (33%) gating modes. GGG-α_{1C} channels displayed only blanks and low-activity gating. These results are consistent with the interpretation that in adult cardiomyocytes $Ca_V\beta$ induces high-P_o gating by stabilizing a continuous helix linking IS6 to AID. Absence of $Ca_V\beta$ binding (as occurs with AID-mutation) reduces the propensity for stabilizing a continuous helix and accordingly decreases fractional occupancy of the high-P_o gating mode. GGG-α_{1C} completely dispels the continuous helix and, therefore, these channels do not sojourn into the high-P_o mode. In the cryo-electron microscopy structure of the homologous $Ca_V1.1$ channel, comparison of the two conformations, class Ia and II, revealed signficant shifts between the C-terminal end of IS6 and I-II helix of the α_1 subunit, and the β subunit [40]. Substitution of the three glycine residues in either one of the two conformations (Figure 6A) likely alters the conformation and increases the flexibility of the I-II loop and the position of the β subunit.

We recently reported that β-adrenergic regulation of cardiac $Ca_V1.2$ channel requires $Ca_V\beta$ binding binding to α_{1C} I-II loop, [13] and PKA phosphorylation of Rad, a small G-protein that inhibits Ca^{2+} channels via binding to $Ca_V\beta$ subunit [15]. Here, we report that GGG-α_{1C} channels expressed in cardiomyocytes, or reconstituted with Rad in heterologous cells, do not display PKA-mediated up-regulation of whole-cell current density, even though they bind $Ca_V\beta$. This result suggests the rigid IS6-AID helical linker is another essential

requirement for transduction of sympathetic regulation of $Ca_V1.2$. The exclusively low-P_o gating mode of GGG-α_{1C} channels is reminiscent of the behavior of Rad-inhibited channels [15]. It is intriguing to speculate that Rad interaction with $Ca_V\beta$ may structurally alter the IS6-AID linker as a mechanism for channel inhibition.

Finally, we examined the impact of the α_{1C} 9*-splice variant that is elevated in the failing heart. Interestingly, the 9*-α_{1C} channels had increased basal P_o and were exclusively recorded in high activity gating modes, with no sojourns into mode 0 gating. Given the proximity of the 9* exon to the AID, and the role of the continuous IS6-AID helix in promoting high activity Cav1.2 gating, one explanation is that the 9* exon may increase basal P_o by further stabilizing the rigid IS6-AID helical linker. Another explanation is that insertion of the 9* exon may affect the function of the voltage-sensor domain of domain II. Previous single-channel experiments have indicated that $Ca_V1.2$ channels in failing hearts have an elevated basal P_o which was putatively attributed to enhanced phosphorylation of the channel [41]. Our results suggest that the increased $Ca_V1.2$ P_o observed in heart failure may be due, in part, to the emergence of the alternatively spliced 9*-α_{1C} variant in this condition.

While powerful tools for electrophysiological assessment of α_{1C} mutants *in vivo*, certain limitations of our transgenic inducible over-expression models prevent examination of whether and how these α_{1C} mutant contribute to both basal and sympathetic regulation of cardiac contractility, and arrhythmogenesis *in vivo*. Chief among these is that same strategy that allows us to isolate the DHP-resistant transgenic channels for electrophysiological assessment *in vivo*—application of nisoldipine—blocks endogenous $Ca_V1.2$ channels in both heart and vasculature, thus leading to hypotension and confounding the experiments. Furthermore, modest over-expression of WT α_{1C} can initiate hypertrophy and heart failure [42, 43]. A direct assessment of whether exon 9* is detrimental could theoretically be achieved with an inducible 9*-α_{1C} knock-in or knock-out strategy, yet due to the genomic structure of exons 9 and 10 in α_{1C}, creating inducible 9*-α_{1C} knock-in or knock-out mice lines would be quite challenging, likely requiring the insertion of a large minigene.

Notwithstanding these limitations, these results provide key insight into the mechanism underlying the β-adrenergic stimulation of Ca^{2+} current and contractility in the heart. β subunit binding to the α_{1C} subunit promotes transitions to a high P_o state. Upon β-adrenergic stimulation, PKA phosphorylation of Rad releases the Rad-induced inhibition of the Ca^{2+} channels (Figure 6B). The Rad-inhibited channels are the heart's functional reserve of Ca^{2+} channels, likely having minimal effects on excitation-contraction coupling at rest, but primed to respond to β-adrenergic agonists upon release of Rad-induced inhibition. Thus, therapeutic release of Rad-mediated inhibition of Ca^{2+} channels could be inotropic.

Supplementary Material

Refer to Web version on PubMed Central for supplementary material.

ACKNOWLEDGEMENTS

Images were collected (and analysed) in the Confocal and Specialized Microscopy Shared Resource of the Herbert Irving Comprehensive Cancer Center at Columbia University, supported by NIH grant P30 CA013696 (National Cancer Institute). Research reported in this publication was performed in the CCTI Flow Cytometry Core, supported in part by the Office of the Director, National Institutes of Health under awards S10RR027050. The content is solely the responsibility of the authors and does not necessarily represent the official views of the National Institutes of Health.

SOURCES OF FUNDING

This work was supported by NIH R01 HL121253, R01 HL126735, R01 HL146149. Arianne Papa was supported by T32HL120826 and NSF 1644869. Jared Kushner was supported by T32 HL007343 and the NY Academy of Medicine Glorney-Raisbeck Fellowship. Jessica Hennessey was supported by T32 HL007854.

Nonstandard Abbreviations and Acronyms:

AID	α-interaction domain
αMHC	α-myosin heavy chain
CaM	calmodulin
DHP	Dihydropyridine
FRET	Förster resonance energy transfer
G-V	conductance-voltage
G_{max}	maximal conductance
HF	heart failure
P_o	open probability
PKA	protein kinase A
pWT	pseudo-wild-type
RGK	Rad, Gem, Kir proteins
rtTA	reverse transcriptional transactivator

REFERENCES

1. Catterall WA. Structure and regulation of voltage-gated ca2+ channels. Annu Rev Cell Dev Biol. 2000;16:521–555 [PubMed: 11031246]
2. Chen YH, Li MH, Zhang Y, He LL, Yamada Y, Fitzmaurice A, Shen Y, Zhang H, Tong L, Yang J. Structural basis of the alpha1-beta subunit interaction of voltage-gated ca2+ channels. Nature. 2004;429:675–680 [PubMed: 15170217]
3. Opatowsky Y, Chen CC, Campbell KP, Hirsch JA. Structural analysis of the voltage-dependent calcium channel beta subunit functional core and its complex with the alpha 1 interaction domain. Neuron. 2004;42:387–399 [PubMed: 15134636]
4. Van Petegem F, Clark KA, Chatelain FC, Minor DL Jr. Structure of a complex between a voltage-gated calcium channel beta-subunit and an alpha-subunit domain. Nature. 2004;429:671–675 [PubMed: 15141227]

5. Perez-Reyes E, Castellano A, Kim HS, Bertrand P, Baggstrom E, Lacerda AE, Wei XY, Birnbaumer L. Cloning and expression of a cardiac/brain beta subunit of the l-type calcium channel. J Biol Chem. 1992;267:1792–1797 [PubMed: 1370480]
6. Singer D, Biel M, Lotan I, Flockerzi V, Hofmann F, Dascal N. The roles of the subunits in the function of the calcium channel. Science. 1991;253:1553–1557 [PubMed: 1716787]
7. Buraei Z, Yang J. The beta subunit of voltage-gated ca2+ channels. Physiol Rev. 2010;90:1461–1506 [PubMed: 20959621]
8. Takahashi SX, Miriyala J, Colecraft HM. Membrane-associated guanylate kinase-like properties of beta-subunits required for modulation of voltage-dependent ca2+ channels. Proc Natl Acad Sci U S A. 2004;101:7193–7198 [PubMed: 15100405]
9. Arias JM, Murbartian J, Vitko I, Lee JH, Perez-Reyes E. Transfer of beta subunit regulation from high to low voltage-gated ca2+ channels. FEBS Lett. 2005;579:3907–3912 [PubMed: 15987636]
10. Findeisen F, Minor DL Jr. Disruption of the is6-aid linker affects voltage-gated calcium channel inactivation and facilitation. J Gen Physiol. 2009;133:327–343 [PubMed: 19237593]
11. Reuter H, Scholz H. The regulation of the calcium conductance of cardiac muscle by adrenaline. J Physiol. 1977;264:49–62 [PubMed: 839456]
12. Bean BP, Nowycky MC, Tsien RW. Beta-adrenergic modulation of calcium channels in frog ventricular heart cells. Nature. 1984;307:371–375 [PubMed: 6320002]
13. Yang L, Katchman A, Kushner J, Kushnir A, Zakharov SI, Chen BX, Shuja Z, Subramanyam P, Liu G, Papa A, Roybal D, Pitt GS, Colecraft HM, Marx SO. Cardiac cav1.2 channels require beta subunits for beta-adrenergic-mediated modulation but not trafficking. J Clin Invest. 2019;129:647–658 [PubMed: 30422117]
14. Finlin BS, Crump SM, Satin J, Andres DA. Regulation of voltage-gated calcium channel activity by the rem and rad gtpases. Proc Natl Acad Sci U S A. 2003;100:14469–14474 [PubMed: 14623965]
15. Liu G, Papa A, Katchman AN, Zakharov SI, Roybal D, Hennessey JA, Kushner J, Yang L, Chen BX, Kushnir A, Dangas K, Gygi SP, Pitt GS, Colecraft HM, Ben-Johny M, Kalocsay M, Marx SO. Mechanism of adrenergic cav1.2 stimulation revealed by proximity proteomics. Nature. 2020;577:695–700 [PubMed: 31969708]
16. Fan J, Fan W, Lei J, Zhou Y, Xu H, Kapoor I, Zhu G, Wang J. Galectin-1 attenuates cardiomyocyte hypertrophy through splice-variant specific modulation of cav1.2 calcium channel. Biochim Biophys Acta Mol Basis Dis. 2019;1865:218–229 [PubMed: 30463690]
17. Tang ZZ, Liao P, Li G, Jiang FL, Yu D, Hong X, Yong TF, Tan G, Lu S, Wang J, Soong TW. Differential splicing patterns of l-type calcium channel cav1.2 subunit in hearts of spontaneously hypertensive rats and wistar kyoto rats. Biochim Biophys Acta. 2008;1783:118–130 [PubMed: 18070605]
18. Liao P, Li G, Yu DJ, Yong TF, Wang JJ, Wang J, Soong TW. Molecular alteration of ca(v)1.2 calcium channel in chronic myocardial infarction. Pflugers Arch. 2009;458:701–711 [PubMed: 19263075]
19. Liao P, Yu D, Lu S, Tang Z, Liang MC, Zeng S, Lin W, Soong TW. Smooth muscle-selective alternatively spliced exon generates functional variation in cav1.2 calcium channels. J Biol Chem. 2004;279:50329–50335 [PubMed: 15381693]
20. Liao P, Zhang HY, Soong TW. Alternative splicing of voltage-gated calcium channels: From molecular biology to disease. Pflugers Arch. 2009;458:481–487 [PubMed: 19151996]
21. Van Petegem F, Duderstadt KE, Clark KA, Wang M, Minor DL Jr. Alanine-scanning mutagenesis defines a conserved energetic hotspot in the cavalpha1 aid-cavbeta interaction site that is critical for channel modulation. Structure. 2008;16:280–294 [PubMed: 18275819]
22. Yang L, Katchman A, Samad T, Morrow JP, Weinberg RL, Marx SO. Beta-adrenergic regulation of the l-type ca2+ channel does not require phosphorylation of alpha1c ser1700. Circ Res. 2013;113:871–880 [PubMed: 23825359]
23. Valencik ML, McDonald JA. Codon optimization markedly improves doxycycline regulated gene expression in the mouse heart. Transgenic Res. 2001;10:269–275 [PubMed: 11437283]
24. Adams PJ, Ben-Johny M, Dick IE, Inoue T, Yue DT. Apocalmodulin itself promotes ion channel opening and ca(2+) regulation. Cell. 2014;159:608–622 [PubMed: 25417111]

25. Banerjee R, Yoder JB, Yue DT, Amzel LM, Tomaselli GF, Gabelli SB, Ben-Johny M. Bilobal architecture is a requirement for calmodulin signaling to cav1.3 channels. Proc Natl Acad Sci U S A. 2018;115:E3026–E3035 [PubMed: 29531055]
26. Hess P, Lansman JB, Tsien RW. Different modes of ca channel gating behaviour favoured by dihydropyridine ca agonists and antagonists. Nature. 1984;311:538–544 [PubMed: 6207437]
27. Schroder F, Handrock R, Beuckelmann DJ, Hirt S, Hullin R, Priebe L, Schwinger RH, Weil J, Herzig S. Increased availability and open probability of single l-type calcium channels from failing compared with nonfailing human ventricle. Circulation. 1998;98:969–976 [PubMed: 9737516]
28. Yang L, Katchman A, Weinberg RL, Abrams J, Samad T, Wan E, Pitt GS, Marx SO. The pdz motif of the alpha1c subunit is not required for surface trafficking and adrenergic modulation of cav1.2 channel in the heart. J Biol Chem. 2015;290:2166–2174 [PubMed: 25505241]
29. Katchman A, Yang L, Zakharov SI, Kushner J, Abrams J, Chen BX, Liu G, Pitt GS, Colecraft HM, Marx SO. Proteolytic cleavage and pka phosphorylation of alpha1c subunit are not required for adrenergic regulation of cav1.2 in the heart. Proc Natl Acad Sci U S A. 2017;114:9194–9199 [PubMed: 28784807]
30. Lee SR, Sang L, Yue DT. Uncovering aberrant mutant pka function with flow cytometric fret. Cell Rep. 2016;14:3019–3029 [PubMed: 26997269]
31. Castellano A, Wei X, Birnbaumer L, Perez-Reyes E. Cloning and expression of a neuronal calcium channel beta subunit. J Biol Chem. 1993;268:12359–12366 [PubMed: 7685340]
32. Lacerda AE, Kim HS, Ruth P, Perez-Reyes E, Flockerzi V, Hofmann F, Birnbaumer L, Brown AM. Normalization of current kinetics by interaction between the alpha 1 and beta subunits of the skeletal muscle dihydropyridine-sensitive ca2+ channel. Nature. 1991;352:527–530 [PubMed: 1650913]
33. Bichet D, Cornet V, Geib S, Carlier E, Volsen S, Hoshi T, Mori Y, De Waard M. The i-ii loop of the ca2+ channel alpha1 subunit contains an endoplasmic reticulum retention signal antagonized by the beta subunit. Neuron. 2000;25:177–190 [PubMed: 10707982]
34. Chien AJ, Zhao X, Shirokov RE, Puri TS, Chang CF, Sun D, Rios E, Hosey MM. Roles of a membrane-localized beta subunit in the formation and targeting of functional l-type ca2+ channels. J Biol Chem. 1995;270:30036–30044 [PubMed: 8530407]
35. Brice NL, Berrow NS, Campbell V, Page KM, Brickley K, Tedder I, Dolphin AC. Importance of the different beta subunits in the membrane expression of the alpha1a and alpha2 calcium channel subunits: Studies using a depolarization-sensitive alpha1a antibody. Eur J Neurosci. 1997;9:749–759 [PubMed: 9153581]
36. Dolphin AC. Beta subunits of voltage-gated calcium channels. J Bioenerg Biomembr. 2003;35:599–620 [PubMed: 15000522]
37. Arikkath J, Campbell KP. Auxiliary subunits: Essential components of the voltage-gated calcium channel complex. Curr Opin Neurobiol. 2003;13:298–307 [PubMed: 12850214]
38. Miriyala J, Nguyen T, Yue DT, Colecraft HM. Role of cavbeta subunits, and lack of functional reserve, in protein kinase a modulation of cardiac cav1.2 channels. Circ Res. 2008;102:e54–64 [PubMed: 18356540]
39. Meissner M, Weissgerber P, Londono JE, Prenen J, Link S, Ruppenthal S, Molkentin JD, Lipp P, Nilius B, Freichel M, Flockerzi V. Moderate calcium channel dysfunction in adult mice with inducible cardiomyocyte-specific excision of the cacnb2 gene. J Biol Chem. 2011;286:15875–15882 [PubMed: 21357697]
40. Wu J, Yan Z, Li Z, Qian X, Lu S, Dong M, Zhou Q, Yan N. Structure of the voltage-gated calcium channel ca(v)1.1 at 3.6 a resolution. Nature. 2016;537:191–196 [PubMed: 27580036]
41. Chen X, Piacentino V 3rd, Furukawa S, Goldman B, Margulies KB, Houser SR. L-type ca2+ channel density and regulation are altered in failing human ventricular myocytes and recover after support with mechanical assist devices. Circ Res. 2002;91:517–524 [PubMed: 12242270]
42. Muth JN, Bodi I, Lewis W, Varadi G, Schwartz A. A ca(2+)-dependent transgenic model of cardiac hypertrophy: A role for protein kinase calpha. Circulation. 2001;103:140–147 [PubMed: 11136699]

43. Wang S, Ziman B, Bodi I, Rubio M, Zhou YY, D'Souza K, Bishopric NH, Schwartz A, Lakatta EG. Dilated cardiomyopathy with increased sr ca2+ loading preceded by a hypercontractile state and diastolic failure in the alpha(1c)tg mouse. PLoS One. 2009;4:e4133 [PubMed: 19125184]

NOVELTY AND SIGNIFICANCE

What Is Known?

- Changing activity of cardiac CaV1.2 channels under basal conditions, during sympathetic activation, and in heart failure is a major determinant of cardiac physiology and pathophysiology.
- Activation of β-adrenergic receptors results in a multi-fold upregulation of $Ca_V1.2$ currents, which is dependent upon PKA phosphorylation of Rad.
- It is unknown how distal conformational changes involving Rad interaction with the $Ca_V\beta$ subunit and phosphorylation-dependent signaling are ultimately conveyed to the channel pore-domain.
- How alternative splicing of the I-II linker of the pore-forming a_{1C} subunit contributes to this regulatory scheme remains to be fully-elucidated.

What New Information Does This Article Contribute?

- Introducing flexibility into the rigid IS6-AID helix markedly reduced basal open probability despite intact binding of $Ca_V\beta$ to α_{1C} I-II loop, and eliminated β-adrenergic agonist stimulation of $Ca_V1.2$ current.
- The α_{1C} 9*-splice variant, which is elevated in the failing human heart, causes an increased basal open probability but did not attenuate stimulatory response to β-adrenergic agonists.
- PKA-modulation of Ca_V channels in heart and HEK cells is dependent on both Rad phosphorylation and a rigid IS6-AID linker

β-adrenergic stimulation of $Ca_V1.2$ current is vital for sympathetic nervous system regulation of cardiac contractility. Recently, we identified Rad, not $Ca_V1.2$, as the functionally-relevant target of PKA. At baseline, Rad inhibits $Ca_V1.2$ by binding to Ca_V β subunit. Upon β-adrenergic activation, PKA phosphorylation of Rad releases this interaction and inhibition. How is the signal from Rad and the β subunit transmitted to the channel's gate? To answer this question, we created transgenic mice featuring the introduction of three glycine residues that disrupt the rigid helix between pore and the α-interaction-domain. Ca^{2+} channels from these mice displayed markedly reduced basal open probability and were insensitive to β-adrenergic agonist stimulation. In contrast, introduction in the α_{1C} I-II loop of the exon 9* splice variant, which is increased in ventricles of patients with end-stage heart failure, increased basal open probability but did not attenuate stimulatory response to β-adrenergic agonists in cardiomyocytes. We speculate that the increased $Ca_V1.2$ open probability observed in heart failure may be due, in part, to the emergence of the alternatively spliced 9*-α_{1C} variant. Taken together, adrenergic stimulation of $Ca_V1.2$ requires an intact rigid linker between the binding site of β subunit in the I-II loop and the channel pore.

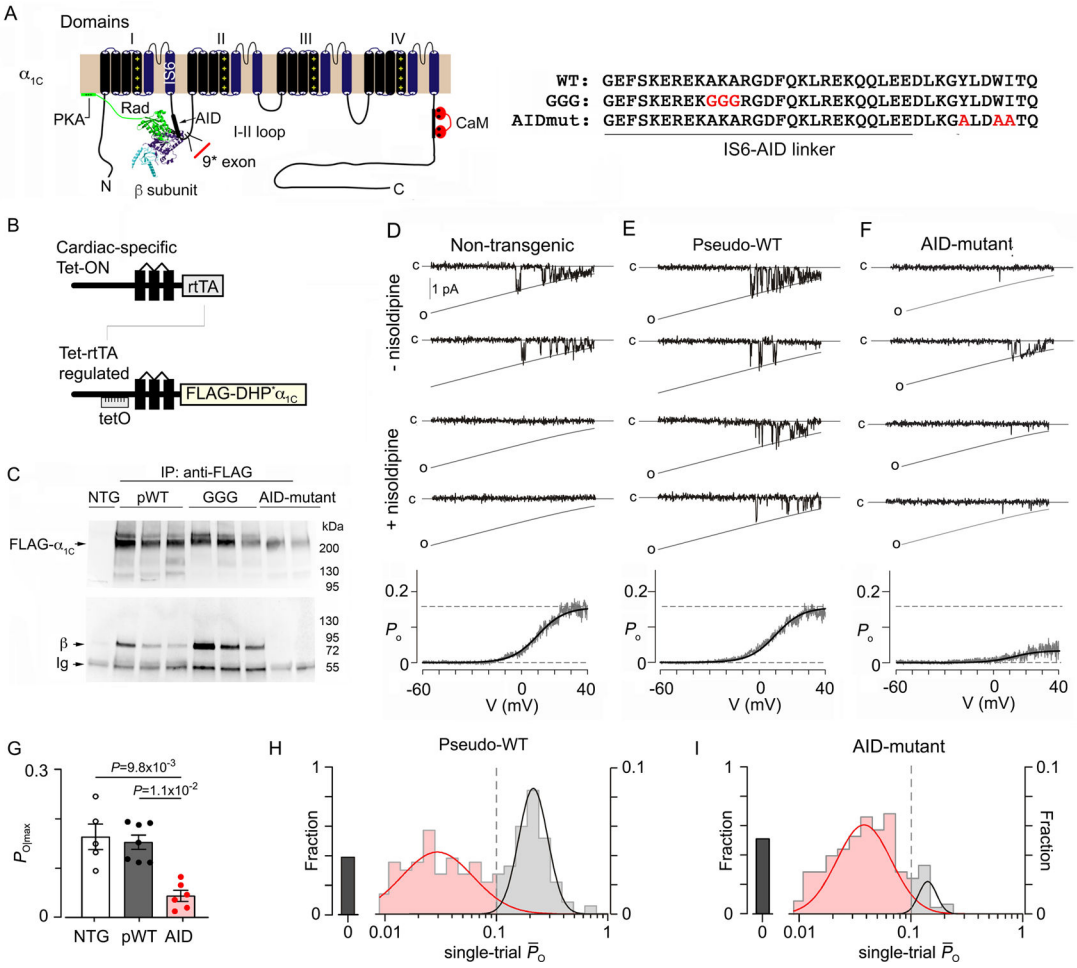

Figure 1. Electrophysiological properties of pseudo-wild-type and AID-mutant Ca^{2+} channels.

(A) Schematic of rabbit cardiac α_{1C} subunit topology showing β subunit binding to α-interaction domain (AID) motif, and the position of the 9* exon in I-II loop. Rad interaction with both β subunit and the plasma membrane are shown. WT, mutant GGG, and mutant AID motif in the I-II loop of α_{1C}. (B) Diagrams showing the binary transgene system that allow expression of FLAG-DHP-resistant (DHP*) α_{1C} only when both reverse tetracycline-controlled transactivator (rtTA) (top diagram) and doxycycline are present (Tet-ON). The lower diagram shows cDNA for FLAG-DHP-resistant (DHP*) α_{1C} ligated behind seven tandem *tetO* sequences. (C) Anti-FLAG (upper) and anti-β immunoblots (lower) of anti-FLAG antibody immunoprecipitation of cardiac homogenates of non-transgenic (NTG), pseudo-wild-type α_{1C}, GGG-α_{1C} and AID-mutant α_{1C} mice. Representative of 3 experiments. (D-F) Single channel Ba^{2+} currents are shown. Channel closures are labeled "c" and openings are downward deflections to the open level (slanted gray curves, labeled "o") in the absence of nisoldipine (top 2 rows) and presence of nisoldipine (bottom 2 rows). Bottom: P_o versus voltage relationship, averaged over multiple patches. N= 5, 7, 6, from left to right. (G) Graph of P_o for Ca^{2+} channels recorded from non-transgenic (NTG), pseudo-wild-type (pWT) α_{1C} and AID-mutant α_{1C} cardiomyocytes. Kruskal-Wallis $P= 4 \times 10^{-4}$; Dunn's multiple comparison test *P*-values in panel. (H-I) Histograms show distribution of

single-trial average P_o obtained from DHP-resistant one-channel patches from pseudo-wild-type α_{1C} and AID-mutant cardiomyocytes.

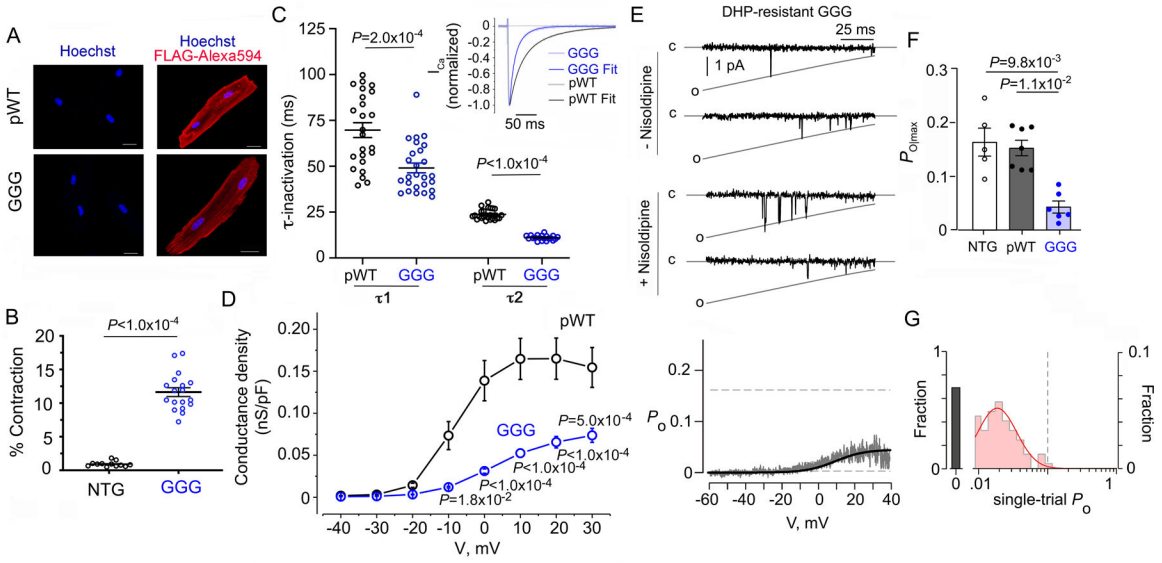

Figure 2. Electrophysiological properties of GGG Ca^{2+} channels.

(A) Immunostaining of pseudo-wild-type (pWT) α_{1C} and GGG-α_{1C} cardiomyocytes. Anti-FLAG and Alexa 594-conjugated secondary antibodies, and nuclear labeling with Hoechst stain. Negative control omitted anti-FLAG antibody. Images obtained with confocal microscopy. Scale bar = 20 μm. (B) Percent contraction of sarcomere length in the presence of nisoldipine for cardiomyocytes isolated from NTG and GGG-α_{1C} mice. Cardiomyocytes were field-stimulated at 1-Hz. Unpaired t-test. (C) Graph of τ_1 and τ_2 inactivation for pseudo-wild-type α_{1C} (n=14 from 4 mice) and GGG-α_{1C} (n=26 from 3 mice) cardiomyocytes. Mann-Whitney test. Inset: Exemplar tracing of normalized Ca^{2+} current in response to a step depolarization to +10 mV. Fits were obtained using two exponentials by Clampfit. (D) Graph of conductance density-voltage relationship for nisoldipine-resistant Ca^{2+} channels recorded from pseudo-wild-type α_{1C} (n=22 from 4 mice) and GGG-α_{1C} (n=20 from 3 mice) cardiomyocytes. Mean ± SEM. $P < 0.0001$ by one-way ANOVA; Sidak's multiple comparison test P-values in panel. (E) Single-channel Ba^{2+} currents in absence and presence of nisoldipine. Bottom: P_o versus voltage relationship averaged over multiple patches. N=6. (F) Graph of P_o for Ca^{2+} channels recorded from non-transgenic (NTG), pseudo-wild-type (pWT) α_{1C}, and GGG α_{1C} cardiomyocytes. NTG and pWT α_{1C} data are the same as in Figure 1. $P = 4 \times 10^{-4}$ by Kruskal-Wallis. Dunn's multiple comparison test P-values in panel. (G) Histogram shows distribution of single-trial average P_o obtained from DHP-resistant one-channel patches from GGG mutant cardiomyocytes.

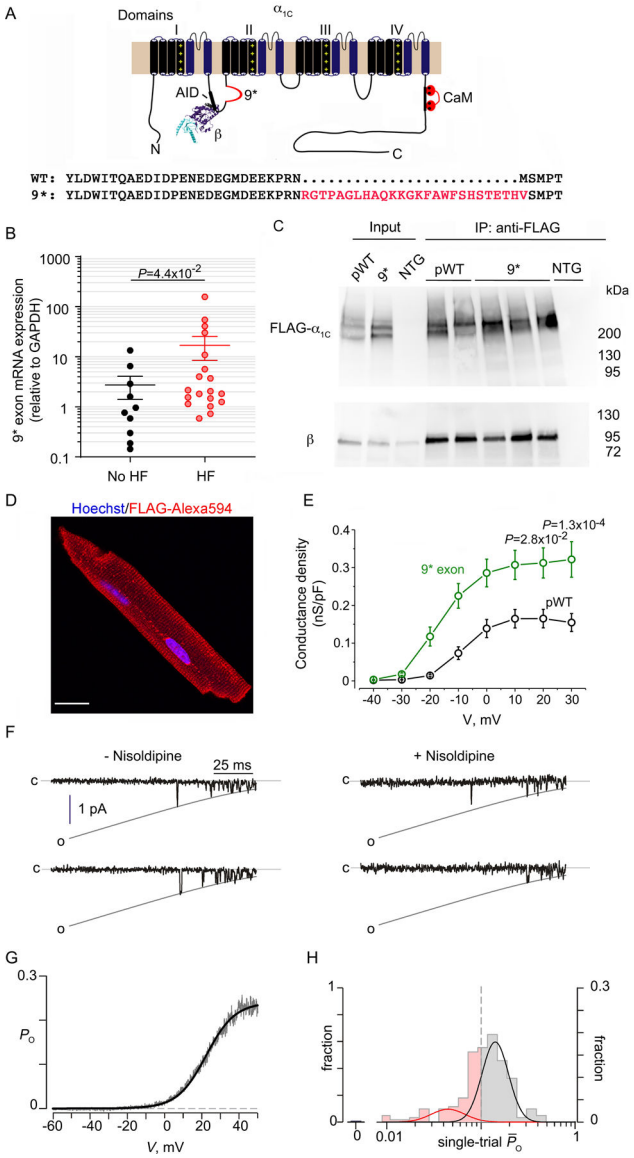

Figure 3. Expression and electrophysiological properties of 9* splice variant-α_{1C} Ca^{2+} channels in heart.

(A) Schematic of rabbit cardiac α_{1C} subunit topology showing β subunit binding to AID motif in I-II loop, and insertion of 9* exon. WT and 9* splice variant sequence in the I-II loop of $\alpha_{1C.}$ (B) Graph of normalized 9* exon mRNA expression from patients with advanced heart failure (HF) undergoing implantation of a left ventricular assist device and control, no-HF patients. Mean ± SEM. N=19 for HF, 10 for no-HF. Mann-Whitney test for *P*-value in panel. (C) Anti-FLAG (upper) and anti-β immunoblots (lower) of anti-FLAG antibody immunoprecipitation of cardiac homogenates of non-transgenic (NTG), 9*-α_{1C} and pseudo-wild-type (pWT) α_{1C} mice. Representative of 3 experiments. Input is 6% of immunoprecipitation. (D) Immunostaining of 9*-α_{1C} cardiomyocyte. Anti-FLAG and Alexa 594-conjugated secondary antibodies, and nuclear labeling with Hoechst stain. Images obtained with confocal microscopy. Scale bar = 20 μm. (E) Graph of conductance density-voltage relationship for nisoldipine-resistant Ca^{2+} channels recorded from pseudo-wild-type

α_{1C} and 9*-α_{1C} cardiomyocytes. pWT α_{1C} curve is the same as in Figure 2D. Mean ± SEM. N= 20 cells from 3 mice. $P < 1.0 \times 10^{-4}$ by one-way ANOVA; Sidak's multiple comparison test *P*-values in panel. (F) Single-channel Ba^{2+} currents in the absence of nisoldipine (left) and presence of nisoldipine (right). (G) P_o versus voltage relationship, averaged over multiple patches. N=10. (H) Histogram shows distribution of single-trial average P_o obtained from DHP-resistant one-channel patches from 9*-expressing cardiomyocytes. These channels largely adopt high P_o gating mode with a marked reduction in the fraction of blank sweeps.

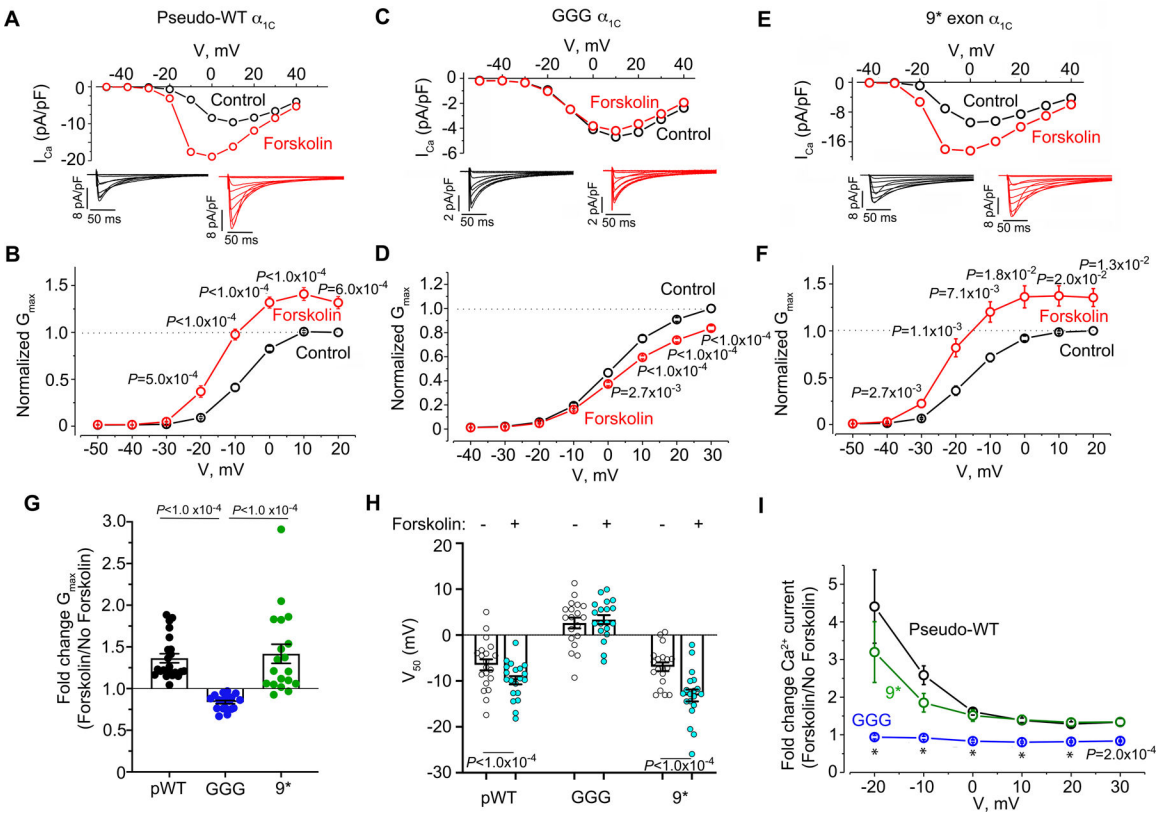

Figure 4. β-adrenergic regulation of GGG and 9* Ca^{2+} channels in cardiomyocytes.

(A, C, E) Current-voltage relationships before and after 10 μM forskolin in the presence of 300 nM nisoldipine. Representative of pseudo-wild-type α_{1C}: n=20, GGG mutant: n= 22 and 9* n=22 cardiomyocytes. Insets: Exemplar whole-cell $Ca_V1.2$ currents recorded from freshly dissociated cardiomyocytes of pseudo-wild-type, GGG and 9* α_{1C} transgenic mice. Pulses from −70 mV to +10 mV before (black traces) and 3 minutes after (red traces) 10 μM forskolin in presence of nisoldipine. (B, D, F) Graphs of conductance density-voltage relationship for nisoldipine-resistant Ca^{2+} channels recorded from pseudo-wild-type α_{1C}, GGG-α_{1C}, and 9*-α_{1C} before (black trace) and after (red trace) forskolin. Mean ± SEM. $P<1.0\times10^{-4}$ by repeated measures ANOVA; Sidak's multiple comparison test P-values are in panels. (G) Fold-change in G_{max}. Shown are means ± SEM; $P<1.0\times10^{-4}$ by Kruskal-Wallis test; Dunn's multiple comparison test P-values in panel. (H) Boltzmann function parameter, V_{50}. Shown are means + SEM; Paired two-tailed t-test. (I) Ratio of Ca^{2+} current after forskolin treatment to Ca^{2+} current before treatment of cardiomyocytes with forskolin for pseudo-wild-type, 9* and GGG-α_{1C} cardiomyocytes. Mean ± SEM. Pseudo-wild-type n=20, GGG mutant: n= 22 and 9* n=22 cardiomyocytes from at least 3 mice for each group. $P<1.0\times10^{-4}$ by Kruskal-Wallis test; Dunn's multiple comparison test P-values in panel for pseudo-WT vs. GGG. * $P<1.0\times10^{-4}$.

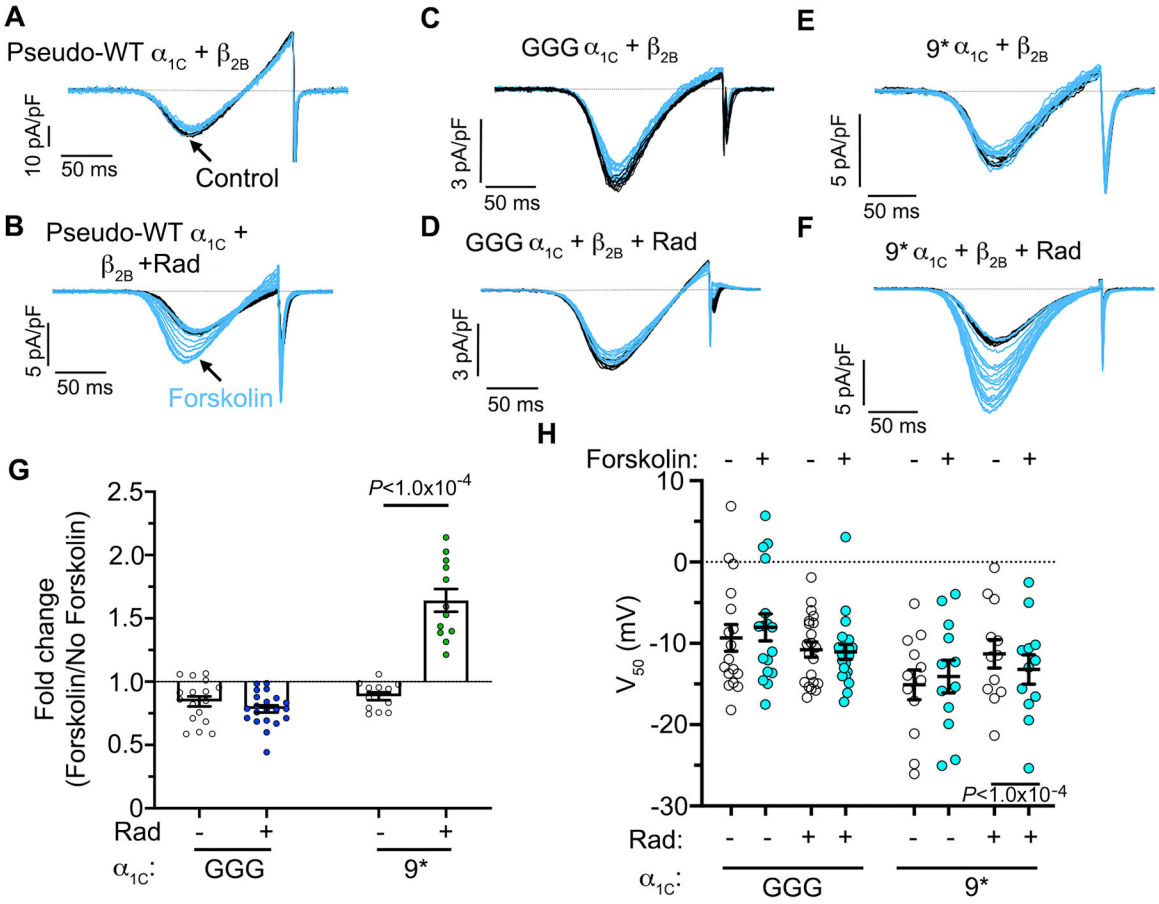

Figure 5. Rad-mediated β−adrenergic regulation of $Ca_V1.2$ requires rigid I-II linker.

(A–F) Ba^{2+} current elicited by voltage ramp every 10 s, with black traces obtained before and blue traces obtained after forskolin. The pseudo-WT (pWT) α_{1C}, β_{2B} and Rad were heterologously expressed in HEK293T cells. Representative of top row: 15, 17, 12 cells, left to right; bottom row: 16, 21, 12 cells, left to right. (G) Fold-change in maximum conductance (G_{max}) induced by forskolin. Mean ± SEM; Two-tailed unpaired *t*-test. (H) Boltzmann function parameter V_{50}. Mean ± SEM; Two-tailed paired *t*-test.

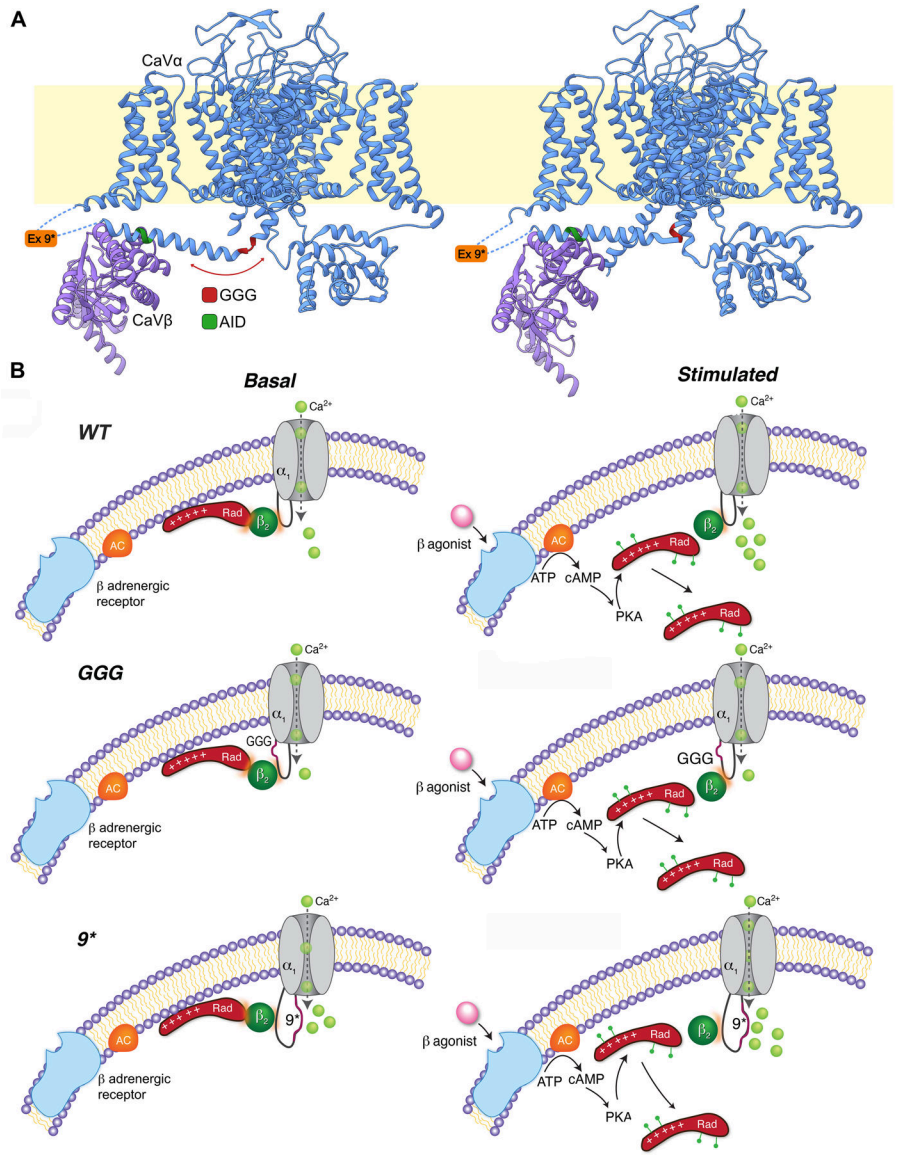

Figure 6. Schematics of role of GGG and 9* in modulating β-adrenergic regulation of $Ca_V1.2$.

(A) Ribbon representation of the published two $Ca_V1.1$ conformations determined by cryo-EM [40] with GGG, AID and exon 9* mutations/insertions in the I-II loop. Left: 5GJV, Right: 5GJW. (B) Proposed models of β−adrenergic regulation of WT, GGG-α_{1C} and 9*-α_{1C} channels. Basal state (left) and after β-adrenergic agonist (stimulated, right). β-agonist-induced activation of adenylyl cyclase (AC) leads to activation of PKA. PKA phosphorylates several residues on Rad, causing dissociationof Rad from the $Ca_V1.2$ complex and therefore increased Ca^{2+} influx. Under basal conditions, the GGG-α_{1C} channels have reduced basal open probability and no response to β-adrenergic stimulation. In contrast to the polyglycine substitution, modifying the I-II loop by introduction of the 9* splice variant increased the basal open probability, yet the stimulatory response to β−adrenergic agonists was preserved.

Major Resources Table

Animals (in vivo studies)				
Species	**Vendor or Source**	**Background Strain**	**Sex**	**Persistent ID / URL**
NA	NA	NA	NA	NA

Genetically Modified Animals					
	Species	**Vendor or Source**	**Background Strain**	**Other Information**	**Persistent ID / URL**
Pseudo-WT-α_{1C}	Mouse	Transgenic Mouse Facility Columbia University	B6CBAF2	Generated at Columbia University	NA
GGG-α_{1C}	Mouse	Transgenic Mouse Facility Columbia University	B6CBAF2	Generated at Columbia University	NA
AID-α_{1C}	Mouse	Transgenic Mouse Facility Columbia University	B6CBAF2	Generated at Columbia University	NA
9*-α_{1C}	Mouse	Transgenic Mouse Facility Columbia University	B6CBAF2	Generated at Columbia University	NA
FVB/N-Tg(Myh6-rtTA)8585Jam/Mmmh	Mouse	MMRC	FVB	NA	RRID: MMRRC_010478-MU

Antibodies					
Target antigen	**Vendor or Source**	**Catalog #**	**Working concentration**	**Lot # (preferred but not required)**	**Persistent ID / URL**
FLAG (rabbit)	Sigma	F7425	1:200 (ICC)		https://www.sigmaaldrich.com/catalog/product/sigma/f7425
Monoclonal Anti-FLAG M2-Peroxidase (HRP) antibody	Sigma	A8592	1:1000 (WB)		https://www.sigmaaldrich.com/catalog/product/sigma/a8592?lang=en&region=US
Beta common (custom)	Yen-Zym		1:1000		epitope: mouse residues 120–138:DSYTSRPS-DSDVSLEEDRE
AlexaFluor 594-goat anti rabbit	Thermo	A11037	1:200	2079421	https://www.thermofisher.com/antibody/product/Goat-anti-Rabbit-IgG-H-L-Highly-Cross-Adsorbed-Secondary-Antibody-Polyclonal/A-11037

DNA/cDNA Clones			
Clone Name	**Sequence**	**Source / Repository**	**Persistent ID / URL**
mouse Rrad mRNA		NCBI/GenBank	XM_006531206
human Xacnb2 mRNA		NCBI/GenBank	NM_201590.3
rabbit cardiac Cacna1c mRNA		NCBI/GenBank	X15539
rabbit smooth muscle Cacna1c mRNA		NCBI/GenBank	X55763

Cultured Cells			
Name	**Vendor or Source**	**Sex (F, M, or unknown)**	**Persistent ID / URL**
HEK293T cells	ATCC		CRL-3216
HEK293 cells	ATCC		CRL-1573

Data & Code Availability		
Description	**Source / Repository**	**Persistent ID / URL**

Other		
Description	**Source / Repository**	**Persistent ID / URL**
polyethylenimine (PEI)	Polysciences	23966-2; https://www.polysciences.com/default/polyethylenimine-linear-mw25000
cycloheximide	Sigma	01810-1G; https://www.sigmaaldrich.com/catalog/product/sigma/c4859?lang=en&region=US
Trypsin 0.05%	Thermo Fisher	25300-054; https://www.thermofisher.com/order/catalog/product/25300054?SID=srch-hj-25300-054#/25300054?SID=srch-hj-25300-054
FBS	Thermo Fisher	10438-026; https://www.thermofisher.com/order/catalog/product/10438026?SID=srch-hj-10438-026#/10438026?SID=srch-hj-10438-026
DMEM	Thermo Fisher	11995-065; https://www.thermofisher.com/order/catalog/product/11995065?SID=srch-hj-11995-065#/11995065?SID=srch-hj-11995-065
Lipofectamine 2000	Thermo Fisher	11668-019; https://www.thermofisher.com/order/catalog/product/11668019?SID=srch-hj-11668-019#/11668019?SID=srch-hj-11668-019
Pen/Strep Glutamine	Thermo Fisher	10378-016; https://www.thermofisher.com/order/catalog/product/10378016?SID=srch-hj-10378-016#/10378016?SID=srch-hj-10378-016
optiMEM	Thermo Fisher	31985-062; https://www.thermofisher.com/order/catalog/product/31985062?SID=srch-hj-31985-062#/31985062?SID=srch-hj-31985-062
Attachment Factor	Thermo Fisher	S-006-100; https://www.thermofisher.com/order/catalog/product/S006100?SID=srch-hj-S-006-100#/S006100?SID=srch-hj-S-006-100
Doxycycline Rodent Diet (200 mg/kg)	Bio Serv	S3888; https://us.vwr.com/store/product/15984109/doxycycline-rodent-diet-sterile-bio-serv
Triton X-100	IBI Scientific	IB07100; https://www.ibisci.com/products/triton-x-100
Calpain inhibitor I	Sigma	A6185; https://www.sigmaaldrich.com/catalog/product/sigma/a6185
Calpain inhibitor II	Sigma	A6060; https://www.sigmaaldrich.com/catalog/product/sigma/a6060
Complete Mini tablets	Roche	04693159001; https://www.sigmaaldrich.com/catalog/product/roche/04693159001?lang=en&region=US
Protein A beads	GE Healthcare	17-0780-01; https://www.sigmaaldrich.com/catalog/product/sigma/ge17078001?lang=en&region=US
Forskolin	Santa Cruz Biotechnology	SC-7562; https://www.scbt.com/p/forskolin-66575-29-9
Isoproterenol	Sigma	I5627; https://www.sigmaaldrich.com/catalog/product/sigma/i5627
Nisoldipine	Santa Cruz Biotechnology	SC-212396; https://www.scbt.com/p/nisoldipine-d7
Amphotericin B	Sigma	A9528; https://www.sigmaaldrich.com/catalog/product/sigma/a9528?lang=en&region=US
SYBR Green qPCR Master Mix	Thermo	https://www.thermofisher.com/order/catalog/product/4309155#/4309155
RNeasy Mini kit	Qiagen	https://www.qiagen.com/us/products/discovery-and-translational-research/dna-rna-purification/rna-purification/total-rna/rneasy-mini-kit/#orderinginformation
High-Capacity cDNA RT kit	Thermo Scientific	https://www.thermofisher.com/order/catalog/product/4368814#/4368814
Red ANTI-FLAG M2 Affinity Gel	Sigma	F2426; https://www.sigmaaldrich.com/catalog/search?term=F2426&interface=All&N=0&mode=match%20partialmax&lang=en&region=US&focus=product

Other		
Description	**Source / Repository**	**Persistent ID / URL**
Liberase	Sigma	5401119001; https://www.sigmaaldrich.com/catalog/product/roche/libtmro?lang=en&region=US